

# A simple mechanism for stable oscillations in an intermediate complexity Earth System Model

ANDREW KEANE\*

School of Mathematical Sciences and Environmental Research Institute,  
University College Cork, Cork, Ireland

ALEXANDRE POHL

Biogéosciences, UMR 6282, UBFC/CNRS, Université Bourgogne Franche-Comté,  
6 boulevard Gabriel, F-21000 Dijon, France

and Department of Earth and Planetary Sciences, University of California, Riverside, CA, USA

HENK A. DIJKSTRA

Institute for Marine and Atmospheric Research Utrecht and Center for Complex Systems  
Studies, Department of Physics, Utrecht University, Utrecht, The Netherlands

ANDY RIDGWELL

Department of Earth and Planetary Sciences, University of California, Riverside, CA, USA

January 2022

arXiv:2201.07883v2 [math.DS] 21 Jan 2022

## Abstract

The global ocean circulation plays a pivotal role in the regulation of the Earth's climate. The specific pattern and strength of circulation also determines how carbon and nutrients are cycled and via the resulting distribution of dissolved oxygen, where habitats suitable for marine animals occur. However, from data and models, transitions in circulation patterns are known to have occurred in the past. Understanding the controls on marine environmental conditions and biological productivity then requires a full appreciation of the nature and drivers of such state transitions. Here we present stable oscillations observed in the ocean circulation of an Earth System Model of intermediate complexity. The presence of the oscillations depends on a circumpolar current. We adapt a simple ocean box model to include a delayed feedback to represent a circumpolar current and investigate stable oscillatory solutions via bifurcation analysis. Our results provide insight into oscillations observed in simulations based on land mass configurations typifying the geological past and also highlight the potential influence of changing circumpolar current speed on the stability of the ocean's meridional overturning circulation.

## 1 Introduction

The ocean circulation plays a critical role in Earth's global climate system, by notably redistributing heat from the low- to high-latitudes and dissolved oxygen from the mixed layer to the deep ocean. It is well known, from both geological proxy data and general circulation models (GCMs), that the ocean circulation has varied through time. It is altered by changes in the geometry of the continents

and the global climatic state [5, 7, 10]. In order to quantify the direction and magnitude of change of the ocean circulation, (paleo)climatologists use Earth System Models, which they run for a few thousand years at a maximum (the ocean mixing timescale). By doing so, it is assumed that the ocean circulation eventually reaches a stable steady state.

Yet, various attempts to run global climate models for a longer time period demonstrated more complex behaviors of the ocean circulation, which sometimes exhibits regimes of stable oscillations. Oscillations have notably been simulated in ocean-only GCMs [20, 30] and ocean GCMs coupled to simple atmospheric components (Earth System Models of intermediate complexity) [11, 8]. To our knowledge, the only study reporting such oscillations based on ocean-atmosphere GCM simulations is the one of Valdes et al. [28], who ran the HadCM3 model for 8,000 years. The absence of further documentation of stable oscillatory regimes in other fully coupled GCMs is not surprising considering that such models are generally run for 2 to 3 thousand years, compared to the  $> 6$  thousand years usually required to identify stable oscillations.

State transitions in ocean circulation simulated in the cGENIE Earth System Model of intermediate complexity, implying regimes of stable oscillations, have recently been demonstrated by Pohl et al. [13]. They have been invoked to explain both the poorly-oxygenated oceans that pervaded several hundreds of millions of years ago [26], when marine life started diversifying in the marine realm [1], and previously enigmatic thousand-year scale cycles identified in marine sediments of the deep geological past [3]. Based on recent studies that pinpoint the tight coupling between marine redox conditions and marine biodiversity [12, 21, 4, 16], the authors conclude that the simulated high-frequency variability in ocean redox conditions would have constituted harsh conditions for the development of

\*corresponding author: [andrew.keane@ucc.ie](mailto:andrew.keane@ucc.ie)

marine life at that time. This study exemplifies the implications that such oscillations have for our understanding of the evolution of both global climate and marine biodiversity, but also highlights the need to better characterize the physical mechanisms causing these oscillations.

Box models have been often used to identify physical mechanisms of oscillatory behavior in the ocean-climate system. Regarding variability of the meridional overturning circulation, two basic types of oscillatory behavior have been identified. Overturning (or loop) oscillations can be found in a four-box model [27] and involve the advective propagation of a buoyancy anomaly along the overturning loop. Such variability is of centennial time scale when only the Atlantic is considered and millennial scale when the global overturning is considered [30]. Oscillatory variability may also be induced by convective processes. The basics of the behavior can be understood from the so-called ‘flip-flop’ oscillation [31], where oscillations between convective and non-convective states occur. The origin of the millennial time scale oscillations, later also referred to ‘deep-decoupling’ oscillations or ‘flushes’ is, however, in more detailed models is best explained by a box model which combines both advective and convective processes [2].

Here, we present a model that reproduces the oscillations obtained in the cGENIE model [13] in a very simple way, by embedding key climatic features in a simple 3-box model. The novel element is that a time delay is introduced, which is an efficient representation of processes occurring in the Southern Ocean.

## 2 cGENIE experiments

To gain insight into the existence of self-sustained oscillations in the ocean circulation, numerical simulations are conducted using the intermediate-complexity Earth System Model cGENIE. cGENIE consists in the coupling between a 3D ocean circulation model and a 2D energy-moisture-balance atmospheric component plus sea-ice module. The model was run on a  $36 \times 36$  equal area grid, with 16 unevenly-spaced vertical levels in the ocean. cGENIE also includes a state-of-the-art representation of marine biogeochemistry. Compared to recent Earth System models of the Coupled Model Intercomparison Project phase 6 (CMIP6), the simplified climatic component of cGENIE offers a rapid model integration time, permitting to run the model for tens of thousands of years.

Pohl et al. [13] recently ran the cGENIE model on various continental configurations characterizing the last 540 millions of years of the geologist past, and noted the existence of stable oscillations under specific combinations of continental configuration and climatic state. Analysis suggests that the existence of an oceanic pole, with no land masses at any longitude, is required to trigger these stable oscillations. However, Pohl et al. [13] focused on the consequences of the resulting state transitions in ocean circulation for ocean oxygenation and the interpretation of geological redox indicators, rather than on the underlying mechanisms of the oscillations. In addition, the experimental setup used by the authors, implying complex land mass configurations and the various feedbacks of cGENIE, renders the analysis complex. As a result, the physical

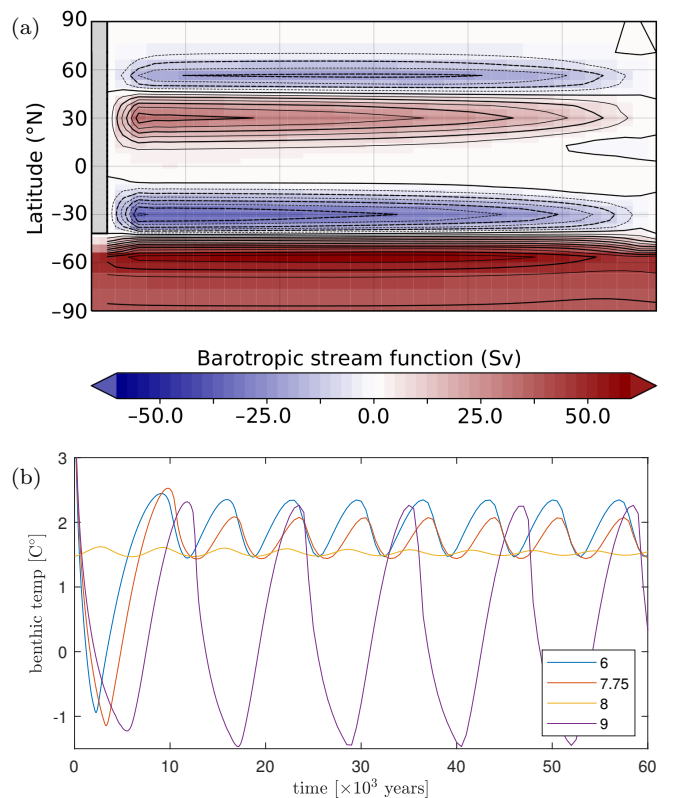


Figure 1: cGENIE experiments. (a) Barotropic streamfunction (Sverdrup,  $1 \text{ Sv} = 10^6 \text{ m}^{-3} \text{ s}^{-1}$ ) for the idealised ocean with a single strip land mass (grey rectangle on left side). Results obtained at  $\times 16 \text{ CO}_2$  ( $\times\text{CO}_2$ , the pre-industrial atmospheric concentration of 280 ppm). The boundary is periodic in the horizontal direction. (b) Example time series of stable oscillations (legend indicates  $\times\text{CO}_2$ ).

mechanisms causing the stable oscillations and state transitions in ocean dynamics in cGENIE remain to be determined.

Here, we undertake a robust analysis of the mechanisms at play by combining new cGENIE experiments conducted with an idealised ocean configuration, and a box model designed specifically to reproduce and identify key characteristics of the cGENIE simulations. Experiments with the idealised model serve as a stepping-stone between results of oscillations in simulations using ‘real-world’ continental configurations [13] and understanding gained through the analysis of simple ocean box models.

Figure 1(a) shows the idealised ocean with a depth of 5km and a single landmass extending southwards to  $45^\circ\text{S}$ . The colours and black contour lines represent the barotropic streamfunction (Sv) as a measure of zonal flow. The most notable feature of the barotropic streamfunction is the strong zonal flow in the southern channel, similar to the Antarctic Circumpolar Current observed in the Earth’s modern continental configuration. It is a wind-driven current that constantly transports water around the pole.

Simulations reveal that for certain levels of atmospheric  $\text{CO}_2$ , stable oscillations may occur with a range of amplitudes, as illustrated in Figure 1(b). However, these stable oscillations cannot be found when the southern channel is

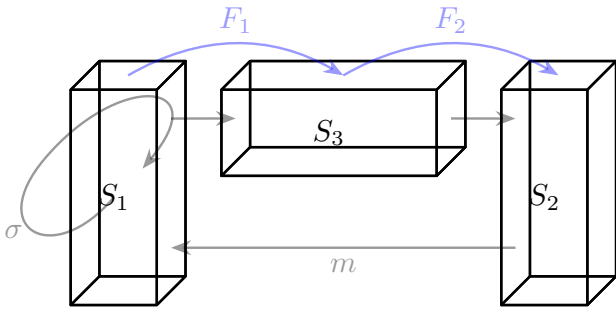


Figure 2: Boxes representing regions of the ocean with salinity variables  $S_{i,1 \leq i \leq 3}$  with arrows representing meridional water flux of strength  $m$  and zonal flux of strength  $\sigma$ . Parameters  $F_1$  and  $F_2$  represent freshwater fluxes.

closed [13].

### 3 Simple box model

A primary question addressed in this paper is: Why do these oscillations appear once the ocean has an open-ocean passage around the south pole? Here, we represent the wind-induced zonal flow due to the open-ocean passage as a delayed feedback in a simple ocean box model and show that this feedback can account for the existence of stable periodic solutions.

We begin with the simplified ocean box model from Ref. [25], which consists of two polar boxes and one upper equatorial box. Assuming salt conservation, the model is written in terms of the salt content of the two polar boxes. We adapt the model to include the effect of zonal transport in the southern channel by including a delayed feedback term. In particular, a parcel of water in the southern polar box will leave its position at time  $t$  and return to the same position at time  $t + \tau$ . The model becomes a set of delay differential equations for the salinity variables  $S_{i \in \{1,2\}}$ :

$$\begin{aligned} V\dot{S}_1 &= S_0 F_1 + m(S_2 - S_1) + \sigma(S_1^\tau - S_1) \\ V\dot{S}_2 &= -S_0 F_2 + m(S_3 - S_2) \end{aligned} \quad (1)$$

Parameters  $F_1$  and  $F_2$  represent surface freshwater fluxes between the boxes. The delayed term is  $S_1^\tau = S_1(t - \tau)$  with delay time  $\tau$  and  $\sigma$  is the feedback strength. The variable  $m$  represents the volume transport between boxes due to density gradients:

$$m = k[\beta(S_2 - S_1) - \alpha T^*]. \quad (2)$$

Parameter  $k$  is a hydraulic constant, while  $\beta$  and  $\alpha$  are salinity and temperature expansion coefficients, respectively. The model assumes a fixed temperature gradient  $T^*$  between the northern and southern boxes. Assuming that salt is conserved, we have  $S_3 = 3S_0 - S_1 - S_2$ . Parameter  $V$  is the (equal) volume of the boxes and  $S_0$  is a reference salinity.

The model is depicted schematically in Figure 2, where positive  $m$  corresponds to clock-wise circulation. Note that

here we only discuss the positive  $m$  solutions, and therefore omit the negative  $m$  equations from the model description.

In this paper we take parameter values from Ref. [25] and let  $k = 23 \times 10^{17} \text{ m}^3 \text{ yr}^{-1}$ ,  $\alpha = 1.7 \times 10^{-4} \text{ K}^{-1}$ ,  $\beta = 0.8 \times 10^{-3} \text{ psu}^{-1}$ ,  $S_0 = 35 \text{ psu}$ , and  $V = 10^{17} \text{ m}^3$ . Furthermore, we set  $F_2 = 1 \text{ Sv}$  ( $10^6 \text{ m}^3 \text{ s}^{-1}$ ). Clearly, this model is very crude in contrast to cGENIE. As such, we do not attempt to find quantitative agreement between the two models. Rather, we demonstrate that this simple model possesses surprisingly rich dynamics and is sufficient for reproducing behaviour observed in cGENIE experiments.

In Ref. [25] the model without the delayed feedback was shown to exhibit, not only the typical bistability between upper ( $m > 0$ ) and lower ( $m < 0$ ) branches of solutions, but also a Bogdanov-Takens bifurcation. This means that instead of the upper branch losing stability at a fold bifurcation, it may for certain values of freshwater flux already lose stability at a Hopf bifurcation, which is always subcritical [24]. The resulting unstable periodic orbits terminate at homoclinic bifurcations.

In the following section, solutions to model (1) and their stability properties are found using the numerical continuation package DDE-Biftool [6, 9, 19, 29].

### 4 Stable oscillations

The solutions to the box model shown in Figure 3 demonstrate how the delayed-feedback effect, due to zonal flow of water in the southern channel, allows the existence of stable periodic orbits. Black curves show the steady-state solutions of  $S_1$  as parameter  $F_1$  is varied, while the blue curves indicate the maximum of  $S_1$  for periodic solutions. Solid and dashed curves indicate stable and unstable solutions, respectively. In panel (a) the parameter  $\sigma$  is set to zero; that is, there is no delayed-feedback effect. In this case, as  $F_1$  increases, the stable steady-state solution loses stability at a subcritical Hopf bifurcation, resulting in a branch of unstable periodic orbits. When the delayed feedback is active, the Hopf bifurcation may become supercritical, resulting in a branch of stable periodic orbits, as shown in panel (b). In this particular example, the stable periodic solutions lose stability at a torus bifurcation before encountering a fold of periodic orbits.

Some readers familiar with control theory may not be surprised by the ability of the delayed feedback to stabilise the pre-existing periodic orbits. Pyragas control, which takes the same mathematical form as the additional term in our model that represents the zonal flow, is used to stabilise unstable periodic orbits as has been demonstrated in many applications, for example, in semiconductor laser experiments [15, 17]. To be precise, the delayed feedback effect in our model is not equivalent to Pyragas control. In the latter, the control is applied to all variables of the system (we only apply it to the salinity in one box) and the delay time is set equal to the period of the unstable periodic orbit to be stabilised. Nonetheless, the method may still be successful for other delay times, as investigated in Ref. [14].

Whether the delayed feedback induces a change in criticality depends on the feedback parameters  $\sigma$  and  $\tau$ . Figure 4 illustrates this dependence, where curves of Hopf

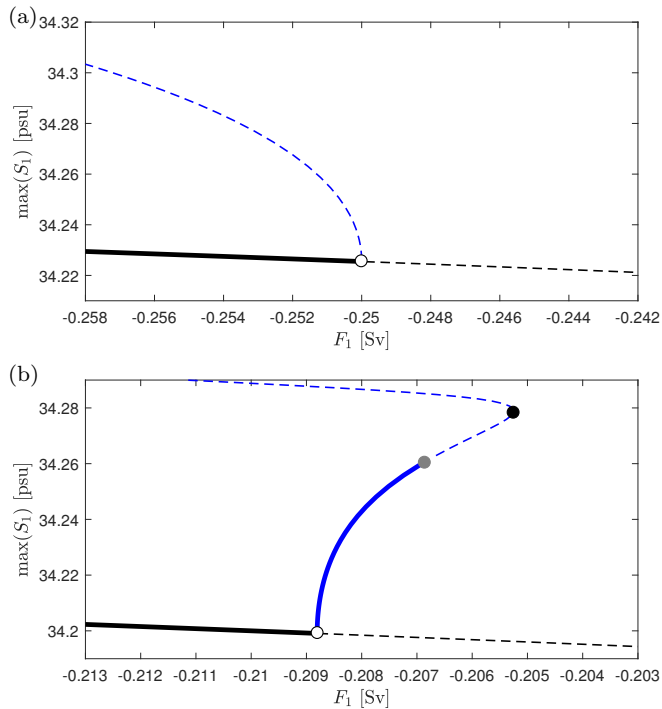


Figure 3: Solutions of model (1) depending on freshwater forcing parameter  $F_1$  for  $T^* = 0$  K. Solid/dashed curves represent stable/unstable solutions. Black are equilibria and blue are maxima of periodic solutions. White, black and grey filled circles represent Hopf, fold and torus bifurcations, respectively. (a) is without the delayed feedback (i.e.  $\sigma = 0$ ), while (b) is with  $\sigma = 11$  Sv. The delay time  $\tau$  is set to 260 years.

bifurcations are calculated in the  $(F_1, \sigma)$ -plane for different values of  $\tau$ . The thick parts of the curves indicate that the Hopf bifurcation is supercritical. Notice that, depending on the feedback strength and delay time, it is possible that the system experiences multiple Hopf bifurcations as  $F_1$  increases.

Figure 5(a) is a bifurcation diagram showing the amplitude of oscillations in terms of mean benthic temperature (i.e. temperature at the bottom level of the ocean) constructed from simulation results of *c*GENIE. Sufficient time is allowed for transient behaviour to die away. Because the simulations take a very long time to run (3 to 4 weeks for a 60-kyr long *c*GENIE simulation as shown in Fig. 1(b)), they are run in parallel for different  $p\text{CO}_2$  levels using the same initial conditions. We observe that as  $p\text{CO}_2$  is increased the steady-state solution loses stability near a  $p\text{CO}_2$  value of  $\times 5$   $p\text{CO}_2$ . The simulations near this bifurcation point demonstrate a square-root growth in amplitude, typical of a supercritical Hopf bifurcation [22]. The family of periodic solutions disappear at another supercritical Hopf bifurcation near  $\times 8$   $p\text{CO}_2$ . The bifurcation point must be very close to  $\times 8$   $p\text{CO}_2$ , since it was necessary to run the simulation for an extremely long time (up to 120 thousand years) while the amplitude of the oscillations continued to decrease very slowly. Finally, the steady-state solution again loses stability after  $\times 8.5$   $p\text{CO}_2$ .

As illustrated in Figure 4 we may choose parameter values so that the system will pass through two supercritical

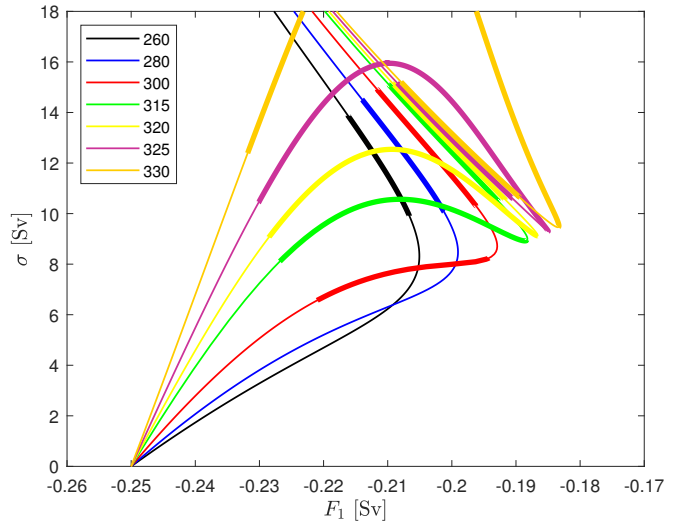


Figure 4: Curves of Hopf bifurcations for  $T^* = 0$  K. At a Hopf bifurcation the equilibrium goes from stable to unstable or unstable to stable and produces a branch of periodic solutions. Where the curves are thin/thick the Hopf bifurcation produces a branch of unstable/stable periodic solutions. The colours refer to different delay times  $\tau$  shown in the legend.

Hopf bifurcations as  $F_1$  increases. Realistically,  $F_1$  is not the only parameter value that would change due to changes in  $p\text{CO}_2$ . Parameters  $F_2$ ,  $T^*$ ,  $\sigma$  and  $\tau$  would all be susceptible to atmospheric changes. Nonetheless, we only consider varying  $F_1$  in an effort to keep the analysis simple and demonstrate qualitative changes in behaviour. Figure 5(b) shows that the effect of the circumpolar current is sufficient for reproducing a family of periodic solutions between two supercritical Hopf bifurcations. In the box model the steady-state solution finally loses stability at a subcritical Hopf bifurcation.

Figure 6(a) is the same as Figure 5(a), only with higher  $\text{CO}_2$  levels. Near  $\times 8.5$   $p\text{CO}_2$  we observe a jump to large-amplitude oscillations, as well as bistability between steady-state and oscillatory solutions. Both the jump to large-amplitude oscillations and bistability are reproduced by the box model in panel (b). Here, the steady-state solution loses stability in a subcritical Hopf bifurcation. The unstable periodic orbits become stable via a fold bifurcation of periodic orbits, before later losing stability at a torus bifurcation.

The termination of the large-amplitude oscillations in Figure 6(a) involves a gradual transition to a state of strong convection at the southern pole. The recreation of transitions between strong and weak convecting states in the box model would require upper and lower boxes, as well as the introduction of an additional convection timescale into the dynamics as in Ref. [2], and is therefore beyond the scope of model (1).

## 5 Discussion

We observe that the delayed feedback provides this simple box model with the capacity to mimic important qualita-

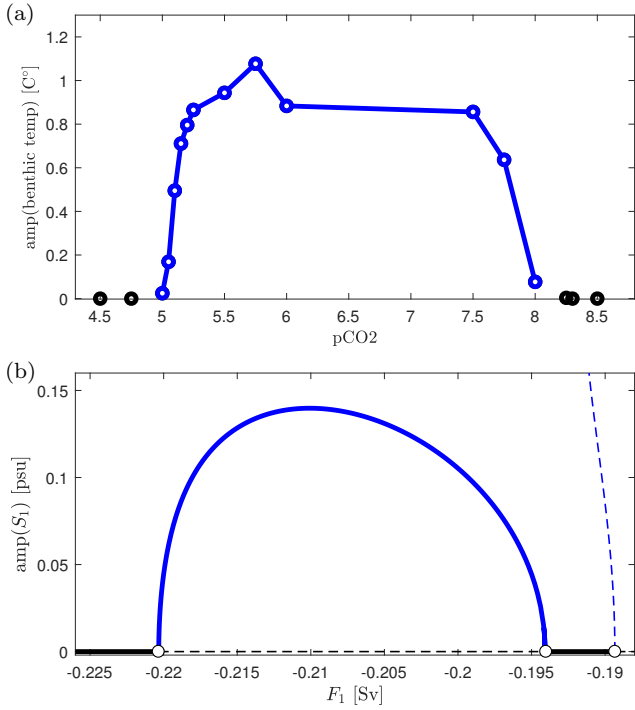


Figure 5: Amplitudes of oscillations with steady-state and periodic solutions shown in black and blue, respectively. (a) cGENIE experiments with varying  $p\text{CO}_2$ . (b) Model (1) solutions while varying  $F_1$  with  $\sigma = 9.5$  Sv,  $\tau = 315$  years and  $T^* = 0$  K. White filled circles represent Hopf bifurcations.

tive behaviour observed in cGENIE experiments using an idealized configuration (Figure 1) and realistic continental configurations of the geological past [13]. Still, there is further significance to these results than providing mechanisms for stable oscillations. It was recently reported that part of the Antarctic Circumpolar Current (ACC) is accelerating due to anthropogenic ocean warming [18]. This would correspond to a shortened delay time in the feedback of model (1).

Figure 7 shows a curve of Hopf bifurcations that demonstrates the sensitivity of an example  $m > 0$  solution ( $F_1 = -0.6$  Sv) to changes in the feedback. Interestingly, it is stable only for intermediate values of feedback strength and delay time. In both scenarios of increasing and decreasing delay time, the solution loses stability at a Hopf bifurcation. For the parameters used in Figure 7, and except for the small segment in bold in the upper-right corner of the figure, the curve of Hopf bifurcations is sub-critical. This corresponds to so-called dangerous tipping events [23], where the system jumps suddenly to a remote state with an alternative circulation pattern. Therefore, the dynamics discussed in this paper is relevant also in a modern context. It is worthwhile to consider the possibility that changes in zonal flow, such as that of the ACC, could play a part in destabilising the meridional overturning circulation of the Atlantic Ocean.

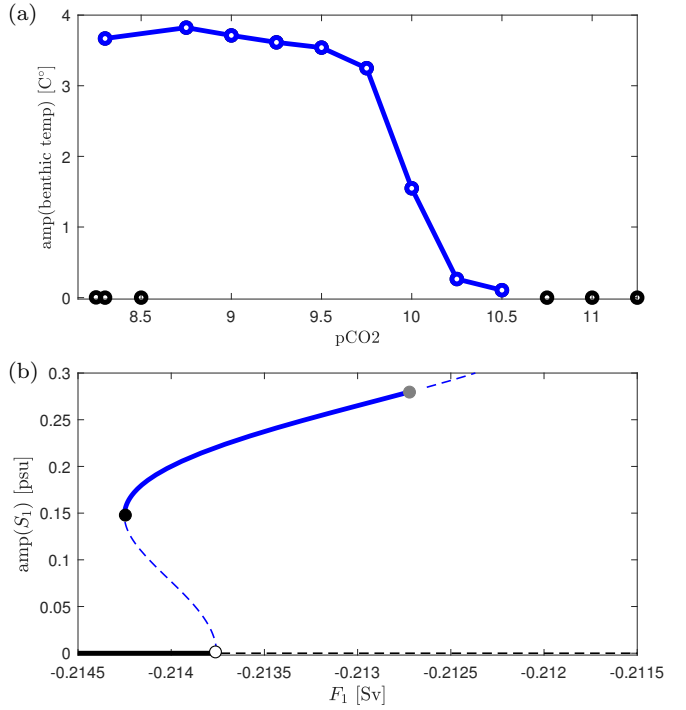


Figure 6: Amplitudes of oscillations with steady-state and periodic solutions shown in black and blue, respectively. (a) cGENIE experiments with varying  $p\text{CO}_2$  with steady-state and periodic solutions shown as black and blue circles, respectively. (b) Model (1) solutions while varying  $F_1$  with  $\sigma = 9$  Sv,  $\tau = 232$  years and  $T^* = 0$  K. White, black and grey filled circles represent Hopf, fold and torus bifurcations, respectively.

## Code Availability

The version of the cGENIE code used in this paper is tagged as release XXX and has a DOI: XXX. Necessary boundary condition files are included as part of the code release. Configuration files for the specific experiments presented in the paper can be found in the installation sub-directory: `genie-userconfigs/MS/keaneetal.journal.2022`. Details of the experiments, plus the command line needed to run each one, are given in the `readme.txt` file in that directory. A manual describing code installation, basic model configuration, and an extensive series of tutorials is provided (DOI: 10.5281/zenodo.5500696).

## Acknowledgments

This project has received funding from the European Union's Horizon 2020 research and innovation programme under the Marie Skłodowska-Curie grant agreement No. 838373 (to AP).

## References

- [1] J Alroy, M Aberhan, D Bottjer, M Foote, F T Fürsich, P J Harries, A J W Hendy, S M Holland, L C Ivany, W Kiessling, M A Kosnik, C R Marshall, A J McGowan, A I Miller, T D Olszewski, M E Patzkowsky, S E Peters, L Villier, P J Wagner, N Bonusco, P S

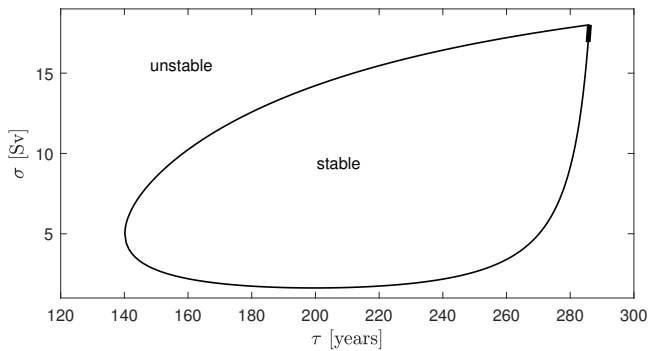


Figure 7: Curve of subcritical (non-bold) and supercritical (bold) Hopf bifurcations in the  $(\sigma, \tau)$ -plane with the stability of the steady state labelled. Parameters are  $F_1 = -0.6$  Sv and  $T^* = 5$  K.

Borkow, B Brenneis, M E Clapham, L M Fall, C A Ferguson, V L Hanson, A Z Krug, K M Layout, E H Leckey, S Nürnberg, C M Powers, J A Sessa, C Simpson, A Tomasovych, and C C Visaggi. Phanerozoic trends in the global diversity of marine invertebrates. *Science*, 321(5885):97–100, 2008.

- [2] A. Colin de Verdière. A Simple Model of Millennial Oscillations of the Thermohaline Circulation. *Journal Of Physical Oceanography*, 37(5):1142–1155, May 2007.
- [3] Tais W. Dahl, Marie Louise Siggaard-Andersen, Niels H. Schovsbo, Daniel O. Persson, Søren Husted, Iben W. Hougård, Alexander J. Dickson, Kurt Kjær, and Arne T. Nielsen. Brief oxygenation events in locally anoxic oceans during the Cambrian solves the animal breathing paradox. *Scientific Reports*, 9(1):1–9, 2019.
- [4] Curtis Deutsch, A Ferrel, Brad Seibel, Hans-Otto Pörtner, and R B Huey. Climate change tightens a metabolic constraint on marine habitats. *Science*, 348(6239):1132–1136, 2015.
- [5] Yannick Donnadiou, Emmanuelle Pucéat, Mathieu Moiroud, François Guillocheau, and Jean François Deconinck. A better-ventilated ocean triggered by Late Cretaceous changes in continental configuration. *Nature Communications*, 7:10316, 2016.
- [6] K. Engelborghs, T. Luzyanina, and G. Samaey. DDE-BIFTOOL: a Matlab package for bifurcation analysis of delay differential equations. *TW Report*, 305, 2000.
- [7] David Ferreira, John Marshall, and Brian Rose. Climate determinism revisited: Multiple equilibria in a complex climate model. *Journal of Climate*, 24(4):992–1012, 2011.
- [8] R. J. Haarsma, J. D. Opsteegh, F. M. Selten, and X. Wang. Rapid transitions and ultra-low frequency behaviour in a 40 kyr integration with a coupled climate model of intermediate complexity. *Climate Dynamics*, 17(7):559–570, 2001.
- [9] Sebastiaan G Janssens. On a normalization technique for codimension two bifurcations of equilibria of delay differential equations. Master’s thesis, 2010.
- [10] Marie Laugié, Yannick Donnadiou, Jean-baptiste Ladant, Laurent Bopp, Christian Ethé, and François Raison. Exploring the impact of Cenomanian paleogeography and marine gateways on oceanic oxygen. *Paleoceanography and Paleoclimatology*, 36(January):e2020PA004202, 2021.
- [11] Katrin J. Meissner, Michael Eby, Andrew J. Weaver, and Oleg A. Saenko. CO2 threshold for millennial-scale oscillations in the climate system: Implications for global warming scenarios. *Climate Dynamics*, 30(2-3):161–174, 2008.
- [12] Justin L Penn, Curtis Deutsch, Jonathan L Payne, and Erik A Sperling. Temperature-dependent hypoxia explains biogeography and severity of end-Permian marine mass extinction. *Science*, 362(6419):eaat1327, 2018.
- [13] Alexandre Pohl, Andy Ridgwell, Richard Stockey, Christophe Thomazo, Andrew Keane, Emmanuelle Vennin, and Christopher Scotese. Plate motion drives variability in ocean oxygenation through the phanerozoic. *Research Square Preprint*, doi: 10.21203/rs.3.rs-915282/v1.
- [14] Anup S Purewal, Claire M Postlethwaite, and Bernd Krauskopf. Effect of delay mismatch in pyragas feedback control. *Physical Review E*, 90(5):052905, 2014.
- [15] Kestutis Pyragas. Continuous control of chaos by self-controlling feedback. *Physics letters A*, 170(6):421–428, 1992.
- [16] Juan G. Rubalcaba, Wilco C.E.P. Verberk, A. Jan Hendriks, Bart Saris, and H. Arthur Woods. Oxygen limitation may affect the temperature and size dependence of metabolism in aquatic ectotherms. *Proceedings of the National Academy of Sciences of the United States of America*, 117(50):31963–31968, 2020.
- [17] S Schikora, HJ Wünsche, and F Henneberger. Odd-number theorem: Optical feedback control at a subcritical hopf bifurcation in a semiconductor laser. *Physical Review E*, 83(2):026203, 2011.
- [18] Jia-Rui Shi, Lynne D Talley, Shang-Ping Xie, Qihua Peng, and Wei Liu. Ocean warming and accelerating southern ocean zonal flow. *Nature Climate Change*, pages 1–8, 2021.
- [19] J. Sieber, K. Engelborghs, T. Luzyanina, G. Samaey, and D. Roose. DDE-BIFTOOL Manual — Bifurcation analysis of delay differential equations. *arXiv preprint arXiv:1406.7144*, 2014.
- [20] Z. Sirkes and E. Tziperman. Identifying a damped oscillatory thermohaline mode in a general circulation model using an adjoint model. *Journal of Physical Oceanography*, 31(8 PART 2):2297–2306, 2001.

- [21] Richard Stockey, Alexandre Pohl, Andy Ridgwell, Seth Finnegan, and Erik A. Sperling. Decreasing Phanerozoic Extinction Intensity Is a Predictable Consequence of Earth Surface Oxygenation and Metazoan Ecophysiology. *Proceedings of the National Academy of Sciences of the United States of America*, 118(41):e2101900118, 2021.
- [22] Steven H Strogatz. *Nonlinear dynamics and chaos with student solutions manual: With applications to physics, biology, chemistry, and engineering*. CRC press, 2018.
- [23] J Michael T Thompson and Jan Sieber. Predicting climate tipping as a noisy bifurcation: a review. *International Journal of Bifurcation and Chaos*, 21(02):399–423, 2011.
- [24] Sven Titz, Till Kuhlbrodt, and Ulrike Feudel. Homoclinic bifurcation in an ocean circulation box model. *International Journal of Bifurcation and Chaos*, 12(04):869–875, 2002.
- [25] Sven Titz, Till Kuhlbrodt, Stefan Rahmstorf, and Ulrike Feudel. On freshwater-dependent bifurcations in box models of the interhemispheric thermohaline circulation. *Tellus A: Dynamic Meteorology and Oceanography*, 54(1):89–98, 2002.
- [26] Rosalie Tostevin and Benjamin JW Mills. Reconciling proxy records and models of Earth’s oxygenation during the Neoproterozoic and Palaeozoic. *Interface focus*, 10(June):20190137, 2020.
- [27] E. Tziperman, J. R. Toggweiler, Y. Feliks, and K Bryan. Instability of the thermohaline circulation with respect to mixed boundary conditions: Is it really a problem for realistic models? *Journal Of Physical Oceanography*, 24:217–232, 1994.
- [28] Paul Valdes, Christopher Scotese, and Dan Lunt. Deep Ocean Temperatures through Time. *Climate of the Past Discussions*, pages 1–37, 2020.
- [29] BI Wage. Normal form computations for delay differential equations in dde-biftool. Master’s thesis, 2014.
- [30] Wilbert Weijer and Henk A. Dijkstra. Multiple oscillatory modes of the global ocean circulation. *Journal of Physical Oceanography*, 33(11):2197–2213, 2003.
- [31] P. Welander. A simple heat-salt oscillator. *Dyn. Atmos. Oceans*, 6:233–242, 1982.